Histopathologic Correlates of Temporal Diffusion Changes in a Rat Model of Cerebral Hypoxia/Ischemia

Naoyuki Miyasaka, Tsukasa Nagaoka, Toshihiko Kuroiwa, Hideaki Akimoto, Tomoko Haku, Toshiro Kubota and Takeshi Aso

AJNR Am J Neuroradiol 2000, 21 (1) 60-66
http://www.ajnr.org/content/21/1/60

AJNR Am J Neuroradiol 21:60–66, January 2000

Histopathologic Correlates of Temporal Diffusion Changes in a Rat Model of Cerebral Hypoxia/Ischemia

Naoyuki Miyasaka, Tsukasa Nagaoka, Toshihiko Kuroiwa, Hideaki Akimoto, Tomoko Haku, Toshiro Kubota, and Takeshi Aso

BACKGROUND AND PURPOSE: **Although diffusion-weighted MR imaging is a powerful tool for evaluating brain ischemia, histopathologic correlates of temporal diffusion changes in cerebral hypoxia/ischemia have not been extensively examined. Diffusion-weighted MR imaging was used to evaluate the relationship between the time course of apparent diffusion coefficient (ADC) changes and the histopathologic findings in cerebral hypoxia/ischemia.**

METHODS: **Thirty 3-week-old rats were subjected to either a 15-, 30-, or 60-minute hypoxic/ischemic insult (unilateral common carotid artery ligation and exposure to 8% oxygen), during and after which diffusion- and T2-weighted MR imaging was performed. Each animal was killed 48 hours or 6 hours after the insult, and fixed sections of the parietal cortex were examined by light microscopy. Ten other (control) rats were subjected to only unilateral common carotid artery ligation or hypoxia.**

RESULTS: **The experimental rats showed three patterns of ADC change, depending on the duration of the hypoxic/ischemic insult: transient (15-minute), biphasic (15-, 30-, or 60-minute), and persistent (60-minute) ADC reduction patterns. The transient ADC reduction pattern (reduction during the insult and recovery after resuscitation) was associated with selective neuronal death. The biphasic and persistent ADC reduction patterns (transient recovery and no recovery after resuscitation, respectively) were associated with cerebral infarction.**

CONCLUSION: **Different temporal patterns of ADC change are associated with different histopathologic findings. Although the clinical manifestations of these different histopathologic presentations are not yet defined, this study indicates that sequential diffusion studies are a potentially powerful tool in the evaluation of hypoxic/ischemic brain injury.**

Cerebral hypoxia/ischemia is a major cause of perinatal brain damage (1). Recently, diffusion-weighted MR imaging has been used for the clinical evaluation of hypoxia/ischemia in neonates (2, 3). This technique enables physicians to detect ischemic brain damage in its very early phase, when ischemic tissue may potentially be responsive to clinical management (4–8). Furthermore, by combining a set of diffusion-weighted MR images obtained under conditions of varying gradient strength, quantitative studies of the apparent diffusion coefficient (ADC) can be obtained (5, 9).

Diffusion-weighted MR imaging has been used to evaluate the pathophysiology of cerebral hypoxia/ischemia and the efficacy of cerebroprotective therapies (10–15). To the best of our knowledge, however, the relationship between the time course of ADC changes and the histopathologic presentation is not known. Thus, it is not clear whether diffusion-weighted MR imaging can be predictive of the histopathologic findings in cerebral hypoxia/ischemia. In this study, we subjected young rats to various durations of cerebral hypoxia/ischemia and compared the ADC changes with the histopathologic appearance. Our purpose was to obtain repeated diffusion-weighted images for the quantitative characterization of diffusion for up to 48 hours after a hypoxic/ischemic insult and to correlate changes in signal intensity on these images with histopathologic findings at 48 hours.

Received April 1, 1999; accepted after revision July 19.

From the Departments of Obstetrics and Gynecology (N.M., T.H., T.Kub., T.A.), Neurosurgery (T.N., H.A.), and Neuropathology (T.Kur.), School of Medicine, Tokyo Medical and Dental University, Japan.

Address reprint requests to Naoyuki Miyasaka, MD, Department of Obstetrics and Gynecology, School of Medicine, Tokyo Medical and Dental University, Yushima 1-5-45, Bunkyo-ku, Tokyo 113-8519, Japan.

Methods

Animal Preparation

The animal experiments were performed in accordance with our institutional guidelines for animal research. In all, 40 3-week-old male Sprague-Dawley rats with an average body weight of 47 ± 5 g (mean ± SD) were used. Anesthesia was

induced with 5% isoflurane and then maintained with 1.5% isoflurane in a mixture of 70% N_2O, 30% O_2 throughout the surgical procedure. Thirty-five of these rats underwent left common carotid artery (CCA) ligation via a ventral transverse cervical incision; the artery was isolated, separated from contiguous structures, ligated in two places, and severed between the ligatures. The other five rats underwent a sham operation that involved just cervical incision and separation of the artery from contiguous structures on the left side. Body temperature was measured using a rectal probe, and the entire surgical procedure lasted less than 5 minutes.

Experimental Protocol

The 40 rats were divided into three groups: group A rats (n = 5) underwent unilateral CCA ligation but not hypoxia, group B rats (n = 5) underwent the sham operation and hypoxia, and group C rats (n = 30) underwent both unilateral CCA ligation and hypoxia. Baseline diffusion-weighted MR imaging was performed, after which the rats in groups B and C were subjected to hypoxia by reducing the inspired oxygen concentration to 8% by N_2 dilution. Diffusion-weighted MR imaging was repeated during the period of hypoxia, and the ADC changes in the ipsilateral cerebral cortex were monitored using ADC maps that were generated as soon as each data acquisition was complete.

The rats in group C were randomly assigned to three groups based on the duration of the hypoxic/ischemic insult: rats in groups C-1 (n = 10), C-2 (n = 10), and C-3 (n = 10) were subjected to 15-, 30-, and 60-minute hypoxic/ischemic insult, respectively. All the rats were resuscitated by increasing the oxygen concentration to 30%. Diffusion-weighted MR imaging was repeated 60 minutes after starting resuscitation, and the rats were returned to their cages after they awoke from anesthesia. Diffusion-weighted MR imaging was performed again 48 hours after the hypoxic/ischemic insult, except for rats that showed severe clinical impairment, who were examined by MR imaging 6 hours after the insult.

The rats in group B (n = 5) were resuscitated 30 minutes after the onset of hypoxia, and were examined by diffusion-weighted MR imaging according to the above protocol. The rats in group A underwent diffusion-weighted MR imaging 1, 2, and 48 hours after unilateral CCA ligation.

Each rat was killed by perfusion of fixative immediately after the final MR imaging examination.

MR Imaging

MR imaging was carried out using a 4.7-T superconducting system with a 33-cm horizontal bore magnet and a 65-mT/m maximum gradient capability (Unity INOVA, Varian, Palo Alto, CA). A quadrature coil with an internal diameter of 8 cm was tuned to 200 MHz for radiofrequency excitation and MR signal reception. After the surgical procedure, each rat was placed in a supine position and body temperature was maintained at 37° ± 0.3°C by a circulating water heating pad placed around the body. Each rat was artificially ventilated with 1.5% isoflurane in a mixture of 70% N_2O and 30% O_2, immobilized with injections of pancuronium bromide (100 mg/kg), and placed in an MR-compatible stereotaxic frame to prevent motion artifacts. The inspired oxygen (FIO_2) and expiratory carbon dioxide (PCO_2) concentrations were monitored continuously throughout the experiment, and the tidal volume was adjusted to produce PCO_2 of 35 to 40 mm Hg.

Diffusion-weighted MR imaging was performed using a multisection, spin-echo sequence with parameters of 1500/80/1 (TR/TE/excitations), a matrix of 128 × 64, a field of view of 30 × 30 mm, and a section thickness of 2 mm without an intersection gap. The diffusion gradients (duration [δ], 30.5 milliseconds; separation time [Δ], 36.7 milliseconds; and gradient strength [G], 0 or 26 mT/m) were applied along the three orthogonal directions (*x*-, *y*-, and *z*-axes). The resulting values for the gradient factor b were 0 or 1200 s/mm^2, and the acquisition time for one set of diffusion-weighted MR images was 6.4 minutes.

Data Analysis

All analyses were performed using a SunSparc 10 workstation (Sun Microsystems, Mountain View, CA) and image analyzing software (XDS, Davis Bioengineering, St. Louis, MO). ADC maps were plotted on a pixel-by-pixel basis using the equation (9)

$$ADC = \ln (S_0/S_1)/(b_1 - b_0)$$

where S_0 and S_1 are the signals of the two diffusion-weighted MR images that represent the average of three orthogonal planes (ie, a trace of diffusion tensor, and b_0 and $b_1 = 0$ and 1200 s/mm^2, respectively). A section 1.8 mm posterior to the bregma was chosen, and regions of interest (ROIs) for the ADC measurements were drawn on the image of the ipsilateral parietal cortex. All data are expressed as the mean ± SD.

Histologic Examination

Immediately after the final MR imaging acquisition procedure, each animal, which was under deep anesthesia, was removed from the MR unit and its brain was fixed by perfusion with a solution of 4% paraformaldehyde in phosphate-buffered saline via an indwelling left ventricular catheter for up to 30 minutes. The brain was then removed, and sequential 2-mm-thick slices corresponding to the MR images were cut and placed in cooled fixative. A slice corresponding to the ADC map 1.8 mm posterior to the bregma was chosen and was prepared and stained with hematoxylin-eosin for light microscopic examination.

Statistical Analysis

ADC values at certain time points were compared with the baseline ADC values for each group by using Student's paired *t*-test. Differences with *P* values of less than .05 were considered significant.

Results

Time Course of ADC Changes

The mean baseline ADC value in the cerebral cortex for all 40 rats was $6.97 \pm 0.4 \times 10^{-4}$ mm^2/s. The control rats (groups A and B) showed neither abnormal signal intensities on T2-weighted images nor ADC changes throughout the period of the experiments. Furthermore, the contralateral parietal cortices of the experimental rats (group C) showed neither abnormal signal intensities on T2-weighted images nor ADC changes throughout the period of the experiments.

The 10 rats subjected to 15 minutes of hypoxia/ischemia (group C-1) showed two patterns of ADC reduction in the ipsilateral parietal cortex: transient (n = 8) and biphasic (n = 2). The transient ADC reduction pattern included acute ADC reduction during the hypoxic/ischemic insult ($4.97 \pm 0.40 \times 10^{-4}$ mm^2/s), recovery to the baseline ADC value 60 minutes after resuscitation ($7.01 \pm 0.48 \times 10^{-4}$ mm^2/s), and no further alteration 48 hours after the insult ($6.99 \pm 0.4 \times 10^{-4}$ mm^2/s). The ADC value during the hypoxic/ischemic insult was significant-

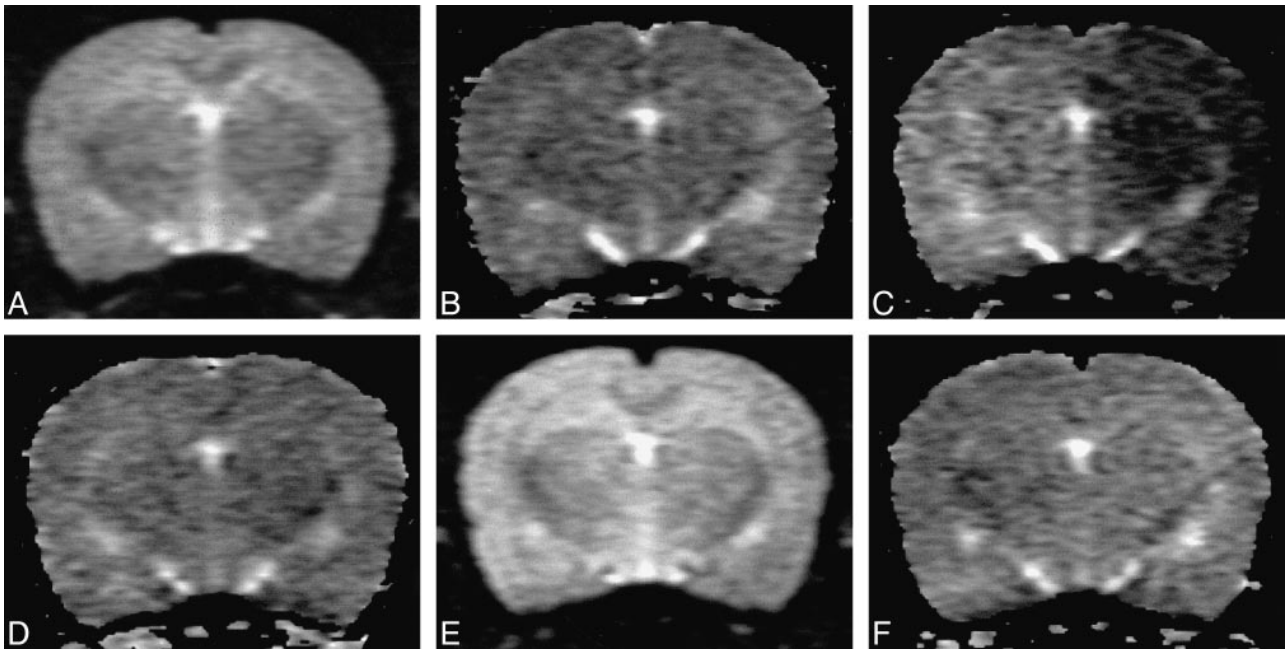

FIG. 1. *A–F,* T2-weighted images (*A* and *E*) and ADC maps (*B, C, D, F*) of a representative rat (group C-1) that showed the transient ADC reduction pattern. T2-weighted images show no abnormal signal intensity at any time. *A,* before the hypoxic/ischemic insult; *E,* 48 hours after the insult. ADC maps show no ADC change before the hypoxic/ischemic insult (*B*), acute ADC reduction in the ipsilateral parietal cortex during the insult (*C*), ADC recovery 60 minutes after resuscitation (*D*), and no ADC change 48 hours after the insult (*F*).

ly lower than the baseline ADC value ($P < .05$), but the ADC values 60 minutes after resuscitation and 48 hours after hypoxic/ischemic insult were not significantly different from the baseline ADC value. In these eight rats, no abnormal signal intensity was observed on T2-weighted images throughout the experiment (Fig 1). The biphasic ADC reduction pattern included acute ADC reduction during the hypoxic/ischemic insult ($3.97 \pm 0.21 \times 10^{-4}$ mm^2/s), transient ADC recovery 60 minutes after resuscitation ($6.98 \pm 0.32 \times 10^{-4}$ mm^2/s), and secondary ADC reduction 48 hours after the insult ($4.38 \pm 0.12 \times 10^{-4}$ mm^2/s). The ADC values during and 48 hours after hypoxic/ischemic insult were significantly lower than the baseline ADC value (both, $P < .05$); but the ADC value 60 minutes after resuscitation was not significantly different from the baseline ADC value. In these two rats, T2-weighted images showed high signal intensity in the affected regions 48 hours after the insult.

All 10 rats subjected to 30 minutes of hypoxia/ischemia (group C-2) showed the biphasic ADC reduction pattern. The ADC values were $4.03 \pm 0.43 \times 10^{-4}$ mm^2/s during the hypoxic/ischemic insult (significantly lower than the baseline ADC value; $P < .05$), $6.96 \pm 0.45 \times 10^{-4}$ mm^2/s 60 minutes after resuscitation (no significant difference from the baseline ADC value), and $4.74 \pm 0.63 \times 10^{-4}$ mm^2/s 48 hours after the insult (significantly lower than the baseline ADC value; $P < .05$). T2-weighted images showed high signal intensity in the affected region 48 hours after the insult (Fig 2).

The 10 rats subjected to 60 minutes of hypoxia/ischemia (group C-3) showed two patterns of ADC reduction: biphasic (n = 4) or persistent (n = 6). The ADC values of the four rats that showed the biphasic ADC reduction pattern were $4.31 \pm 0.15 \times 10^{-4}$ mm^2/s during the hypoxic/ischemic insult (significantly lower than the baseline ADC value; $P < .05$), $7.06 \pm 0.39 \times 10^{-4}$ mm^2/s 60 minutes after resuscitation (no significant difference from the baseline ADC value), and $4.25 \pm 0.69 \times 10^{-4}$ mm^2/s 48 hours after the insult (significantly lower than the baseline ADC value; $P < .05$). The T2-weighted images of these four rats showed high signal intensity in the affected region 48 hours after the insult. The other six rats showed the persistent ADC reduction pattern: an ADC decrease during the hypoxic/ischemic insult ($3.93 \pm 0.28 \times 10^{-4}$ mm^2/s) and a further decrease 60 minutes after resuscitation ($2.98 \pm 0.39 \times 10^{-4}$ mm^2/s). The ADC values during the insult and 60 minutes after resuscitation were significantly lower than the baseline ADC value (both, $P < .05$). Each of these six rats showed severe clinical impairment after they awoke from anesthesia and they died within 24 hours of the hypoxic/ischemic insult. High signal intensities on T2-weighted images and sustained ADC decreases were seen 6 hours after the insult in these six rats. At that time, large and midline shifts, caused by swelling of the ipsilateral cerebral hemisphere, were observed in the affected regions (Fig 3).

The mean ADC values at the end of the hypoxic/ischemic insult were $4.97 \pm 0.40 \times 10^{-4}$ mm^2/s, $4.08 \pm 0.37 \times 10^{-4}$ mm^2/s, and $3.93 \pm 0.28 \times 10^{-4}$ mm^2/s in the rats with the transient, biphasic, and persistent ADC reduction patterns, respective-

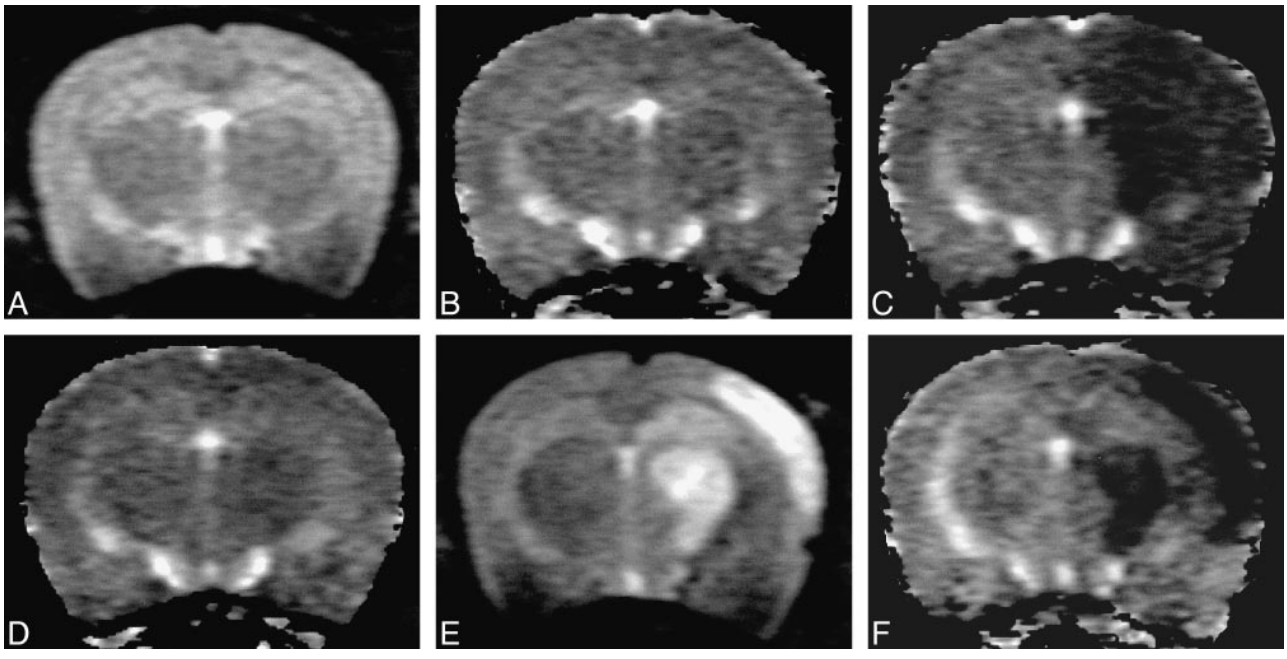

FIG. 2. *A–F,* T2-weighted images (*A* and *E*) and ADC maps (*B, C, D, F*) of a representative rat (group C-2) that showed the biphasic ADC reduction pattern. T2-weighted images show no abnormal signal intensity before the hypoxic/ischemic insult (*A*), during the insult, or 60 minutes after resuscitation; they do show high signal intensity in the ipsilateral parietal cortex 48 hours after the insult (*E*). ADC maps show no ADC change before the hypoxic/ischemic insult (*B*), acute ADC reduction in the ipsilateral parietal cortex during the insult (*C*), ADC recovery 60 minutes after resuscitation (*D*), and secondary ADC reduction in the ipsilateral parietal cortex 48 hours after the insult (*F*).

ly. The mean ADC value at the end of the hypoxic/ischemic insult in the rats with the transient ADC reduction pattern was significantly higher than that in the rats with the biphasic or permanent ADC reduction patterns ($P < .01$), whereas there was no significant difference in ADC values between the rats with the biphasic or permanent ADC reduction patterns.

Relationship between ADC Changes and Histopathologic Findings

The time course of the ADC changes and the histopathologic findings of each group are summarized in the Table. The control rats showed no ADC changes (n = 10) and their histopathologic examinations showed that neurons were intact and that the cell density was well preserved (Fig 4A), whereas the rats with the transient ADC reduction pattern (n = 8) invariably showed neuronal loss with ischemic changes (cytoplasmic eosinophilia and pyknotic nuclei), which indicated selective neuronal death. In these rats, pan-necrosis was not found, but more than half of the neurons showed selective neuronal death (Fig 4B). Rats with the biphasic ADC reduction pattern (n = 16) showed pan-cellular necrosis, indicative of cerebral infarction on histopathologic examination (Fig 4C); and the rats with the persistent ADC reduction pattern (n = 6) showed a large hemispheric infarction, as evidenced by extensive neuronal pyknosis and severe neuropilar microvacuolation 6 hours after the hypoxic/ischemic insult (Fig 4D).

Thus, our data clearly reveal a close association between the time course of ADC changes and the histopathologic findings in the ipsilateral parietal cortex after hypoxic/ischemic insult.

Discussion

We exposed young rats to unilateral CCA ligation and hypoxia, which is an established model of cerebral hypoxia/ischemia (16). Using this model, we compared the time course of ADC changes with the histopathologic findings in cerebral hypoxia/ischemia. Acute ADC reduction during the early phase of ischemia has been reported to be associated with cell swelling resulting from ischemia-induced energy failure (4, 8). Recent reports on experimental and human brain ischemia have shown that early reperfusion can reverse acute ADC reductions and that diffusion-weighted MR imaging delineates not only irreversible but also potentially reversible ischemic brain changes (17–19). In this regard, we found three time-course patterns of ADC changes, which depended on the duration of the hypoxic/ischemic insult: the transient, biphasic, and persistent ADC reduction patterns.

The severity of insult in this hypoxia/ischemia model has been modified by varying the duration of hypoxia (20), but a large variation in the extent of brain injury is known to occur even after the same duration of insult (21). This variation may be due to interindividual variability in susceptibility to hypoxia. We found different ADC reduction patterns and histopathologic presentations among the

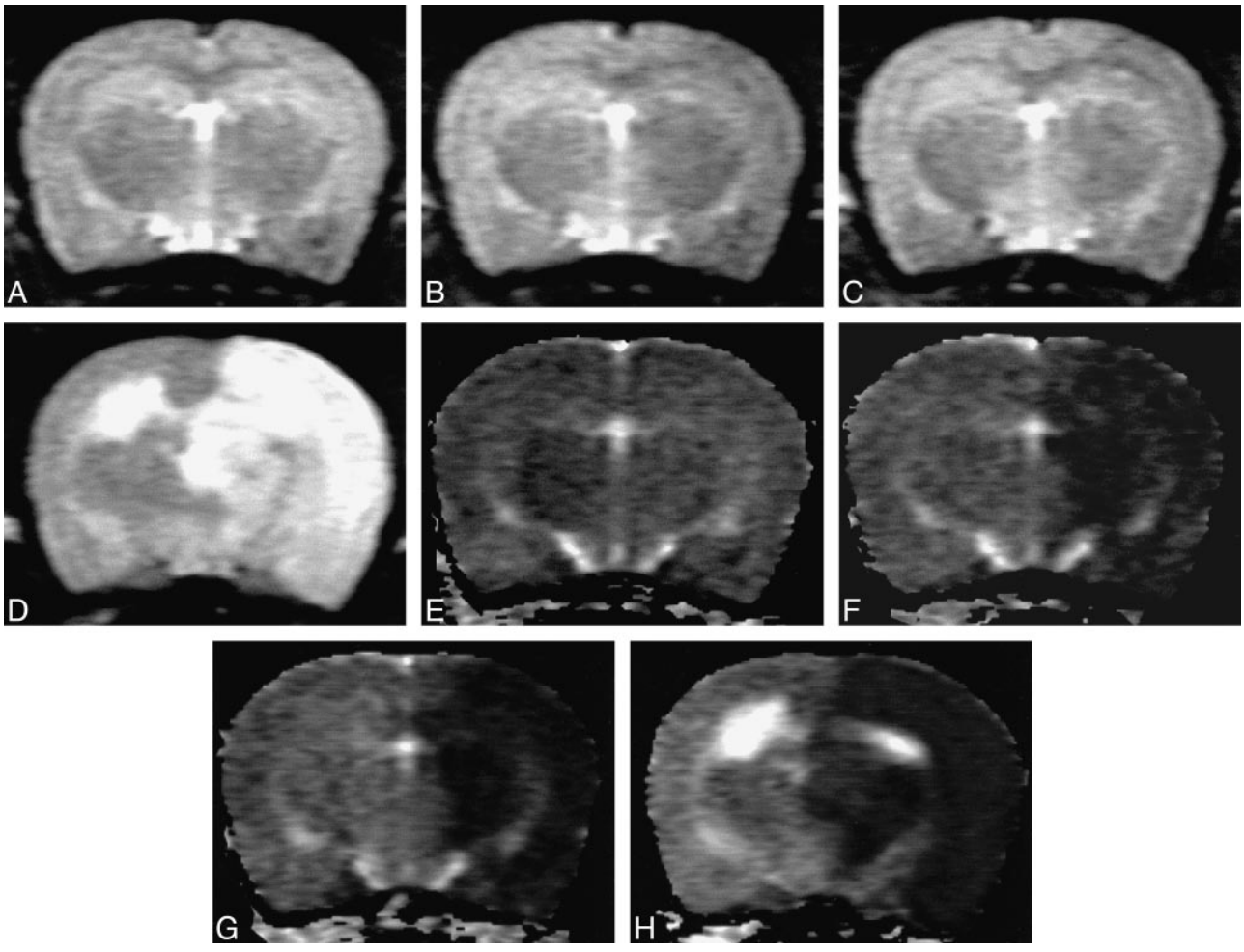

FIG. 3. *A–H,* T2-weighted images (*A–D*) and ADC maps (*E–H*) of a representative rat (group C-3) that showed the persistent ADC reduction pattern.

A–D, T2-weighted images show no abnormal signal intensity before the hypoxic/ischemic insult (*A*), during the insult (*B*), or 60 minutes after resuscitation (*C*); they do show high signal intensity in the ipsilateral parietal cortex 6 hours after the insult (*D*).

E–H, ADC maps show no ADC change before the hypoxic/ischemic insult (*E*), acute ADC reduction in the ipsilateral parietal cortex during the insult (*F*), and sustained ADC decrease 60 minutes after resuscitation (*G*) and 6 hours after the insult (*H*).

Time course of ADC changes and histopathologic findings in the ipsilateral parietal cortex in a rat model of hypoxia/ishemia

Group	No.	CCA Ligation	Hypoxia	ADC Reduction Pattern	Histopathologic Finding
A	5	Yes	None	No change	Normal
B	5	No	30 min	No change	Normal
C-1	8	Yes	15 min	Transient	SND
C-1	2	Yes	15 min	Biphasic	Infarction
C-2	10	Yes	30 min	Biphasic	Infarction
C-3	4	Yes	60 min	Biphasic	Infarction
C-3*	6	Yes	60 min	Persistent	Massive infarction†

Note.—CCA indicates common carotid artery; SND, selective neuronal death.

* Histopathologic examination was performed 6 h after the insult because these rats showed severe clinical impairment and died within 24 h.

† A large hemispheric infarction with a midline shift.

rats subjected to the same hypoxic/ischemic insult. Our data, however, clearly show a close relationship between the time course pattern of ADC changes and the histopathologic findings in cerebral hypoxia/ischemia.

Transient ADC reduction was seen in eight of 10 rats subjected to hypoxia/ischemia for 15 minutes. As expected from previous reports (17, 18), no cerebral infarction was found in rats with the transient ADC reduction pattern; however, neurons in the ipsilateral parietal cortices of these rats consistently showed selective neuronal death 48 hours after the hypoxic/ischemic insult. This finding is important because such neuronal injury can cause neurode-

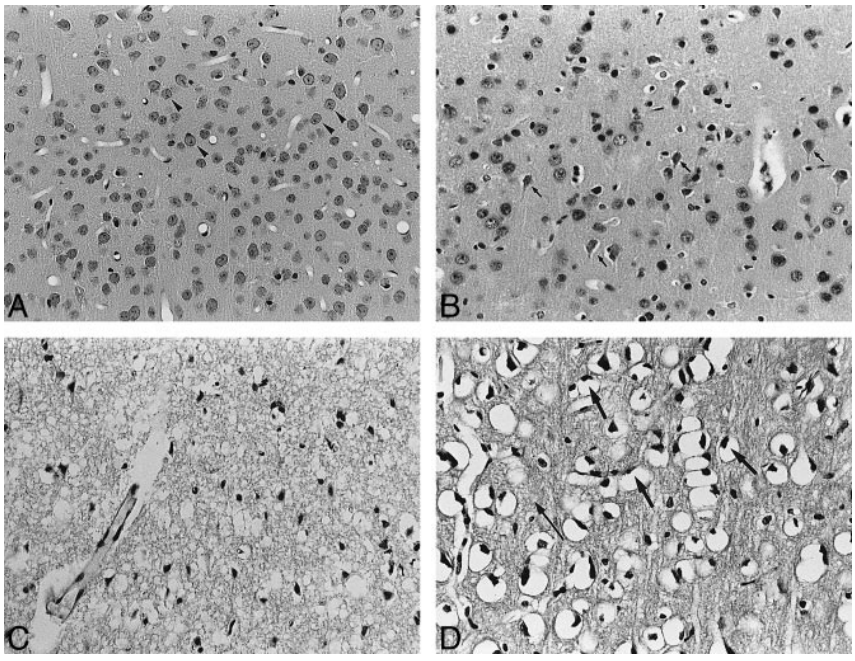

FIG. 4. Histopathologic findings of the ipsilateral parietal cortices of the control and experimental rats (H and E, original magnification ×400).

A, Light micrograph of a parietal cortex section from a control rat (group A) shows intact neurons (*arrowheads*) and well-preserved cell density 48 hours after CCA ligation.

B, Light micrograph of a parietal cortex section from a rat with the transient ADC reduction pattern (group C-1) shows neuronal loss with ischemic changes (cytoplasmic eosinophilia and pyknotic nuclei, *arrows*) 48 hours after the hypoxic/ischemic insult.

C, Light micrograph of a parietal cortex section from a rat with the biphasic ADC reduction pattern (group C-2) shows pancellular necrosis, indicative of cerebral infarction, 48 hours after the hypoxic/ischemic insult.

D, Light micrograph of a parietal cortex section from a rat with the persistent ADC reduction pattern (group C-3) shows cerebral infarction with extensive neuronal pyknosis (*thick arrows*) and severe neuropilar microvacuolation (*thin arrow*) 6 hours after the hypoxic/ischemic insult.

velopmental disabilities, depending on the number of injured neurons. Neuronal death after cerebral hypoxia/ischemia has been reported to present as two different modes of cell death: necrosis and apoptosis (22). Necrosis predominates in more intense forms of ischemic damage, whereas apoptosis occurs in milder forms of ischemic damage (23). Delayed neuronal death is also a well-known phenomenon after a brief period of brain ischemia (24). In this study, we did not look for apoptosis or histopathologic changes earlier than 48 hours after the hypoxic/ischemic insult unless the rat showed severe clinical impairment, and we did not determine when or how the neuronal damage occurred in the rats with the transient ADC reduction pattern. Our data, however, show that ADC normalization after a short period of hypoxic/ischemic insult does not always correlate with neuronal salvage. Therefore, we speculate that once ADC reduction is caused by cerebral hypoxia/ischemia, not only resuscitation but also additional cerebroprotective therapy may be effective to reduce selective neuronal death.

The biphasic ADC reduction pattern was seen in two of 10 rats subjected to 15 minutes of hypoxia/ischemia, in all 10 of the rats subjected to 30 minutes of hypoxia/ischemia, and in four of the 10 rats subjected to 60 minutes of hypoxia/ischemia. Secondary ADC reduction is a well-known occurrence (11–13), and this appeared to be analogous to the biphasic energy failure that has been measured by phosphorous nuclear MR spectroscopy in cerebral hypoxia/ischemia (25–27). All the rats with the biphasic ADC reduction pattern showed pan-cellular necrosis, which is indicative of cerebral infarction. The persistent ADC reduction pattern, seen in six of the 10 rats subjected to 60 minutes of hypoxia/ischemia, was associated with massive infarction with a midline shift and early death of the animal. The rats with biphasic or persistent ADC reduction patterns showed high signal intensity on T2-weighted images in the affected regions 48 hours and 6 hours after the insult, respectively. These findings demonstrate that high signal intensity on T2-weighted images is indicative of irreversible brain damage in cerebral hypoxia/ischemia.

Conclusion

We found three different time course patterns of ADC changes, depending on the duration of the hypoxic/ischemic insult: the transient, biphasic, and persistent ADC reduction patterns. The transient pattern correlated with selective neuronal death, whereas the biphasic and persistent patterns were associated with cerebral infarction that finally showed high signal intensity on T2-weighted images. Although the clinical manifestations of these different histopathologic findings are not yet defined, this study indicates that sequential diffusion studies are a potentially powerful tool in the evaluation of hypoxic/ischemic brain injury.

Acknowledgments

We are grateful for the helpful contributions and support of Prof. K. Hirakawa during this project.

References

1. Volpe JJ. ***Neurology of the Newborn.*** 3rd ed. Philadelphia: Saunders; 1994: 279–313

2. Cowan FM, Pennock JM, Hanrahan JD, Manji KP, Edwards AD. **Early detection of cerebral infarction and hypoxic ischemic encephalopathy in neonates using diffusion-weighted magnetic resonance imaging.** *Neuropediatrics* 1994;25:172–191
3. Toft PB, Leth H, Peitersen B, Lou HC, Thomsen C. **The apparent diffusion coefficient of water in gray and white matter of the infant brain.** *J Comput Assist Tomogr* 1996;20:1006–1011
4. Benveniste H, Hedlund LW, Johnson GA. **Mechanism of detection of acute cerebral ischemia in rats by diffusion-weighted magnetic resonance microscopy.** *Stroke* 1992;23:746–754
5. Moseley ME, Kucharczyk J, Mintorovitch J, et al. **Diffusion-weighted MR imaging of acute stroke: correlation with T2-weighted and magnetic susceptibility-enhanced MR imaging in cats.** *AJNR Am J Neuroradiol* 1990;11:423–429
6. Moseley ME, Cohen Y, Mintorovitch J, et al. **Early detection of regional cerebral ischemia in cats: comparison of diffusion- and T2-weighted MRI and spectroscopy.** *Magn Reson Med* 1990;14:330–346
7. Allen KL, Busza AL, Gadian DG. **A diffusion-weighted proton magnetic resonance imaging study of cerebral ischemia in the gerbil.** *J Cereb Blood Flow Metab* 1993;13:S312
8. Busza AL, Allen KL, King MD, van Bruggen N, Williams SR, Gadian DG. **Diffusion-weighted imaging studies of cerebral ischemia in gerbils: potential relevance to energy failure.** *Stroke* 1992;23:1602–1612
9. Le Bihan D, Breton E, Lallemand D, Aubin ML, Vignaud J, Laval-Jeantet M. **Separation of diffusion and perfusion in intravoxel incoherent motion MR imaging.** *Radiology* 1988;168:497–505
10. Rumpel H, Buchli R, Gehrmann J, Illi O, Martin E. **Magnetic resonance imaging of brain edema in the neonatal rat: a comparison of short and long term hypoxia-ischemia.** *Pediatr Res* 1995;38:113–118
11. Rumpel H, Nedelcu J, Aguzzi A, Martin E. **Late glial swelling after acute cerebral hypoxia-ischemia in the neonatal rat: a combined magnetic resonance and histochemical study.** *Pediatr Res* 1997;42:54–59
12. Dijkhuizen RM, Knollema S, van der Worp HB, et al. **Dynamics of cerebral tissue injury and perfusion after temporary hypoxia-ischemia in the rat: evidence for region-specific sensitivity and delayed damage.** *Stroke* 1998;29:695–704
13. Thornton JS, Ordidge RJ, Penrice J, et al. **Temporal and anatomical variations of brain water apparent diffusion coefficient in perinatal cerebral hypoxic-ischemic injury: relationships to cerebral energy metabolism.** *Magn Reson Med* 1998;39:920–927
14. D' Ardeuil HE, de Crespigny AJ, Roether J, et al. **Diffusion and perfusion magnetic resonance imaging of the evolution of hypoxic ischemic encephalopathy in the neonatal rabbit.** *J Magn Reson* 1998;8:820–828
15. Tuor UI, Kozlowski P, Del Bigio MR, et al. **Diffusion- and T2-weighted increases in magnetic resonance images of immature brain during hypoxia-ischemia: transient reversal posthypoxia.** *Exp Neurol* 1998;150:321–328
16. Rice JE III, Vannucci RC, Brierly JB. **The influence of immaturity on hypoxic-ischemic brain damage in the rat.** *Ann Neurol* 1981;9:131–141
17. Minematsu K, Li L, Sotak CH, Davis MA, Fisher M. **Reversible focal ischemic injury demonstrated by diffusion-weighted magnetic resonance imaging in rats.** *Stroke* 1992;23:1304–1311
18. Hasegawa Y, Fisher M, Latour LL, Dardzinski BJ, Sotak CH. **MRI diffusion mapping of reversible and irreversible ischemic injury in focal brain ischemia.** *Neurology* 1994;44:1484–1490
19. Miyabe M, Mori S, van Zijl PCM, et al. **Correlation of the average water diffusion constant with cerebral blood flow and ischemic damage after transient middle cerebral artery occlusion in cats.** *J Cereb Blood Flow Metab* 1996;16:381–391
20. Towfighi J, Yager JY, Housman C, Vannucci RC. **Neuropathology of remote hypoxic-ischemic damage in the immature rat.** *Acta Neuropathol* 1991;81:578–587
21. Hagberg H, Bona E, Gilland E, Puka-Sundvall M. **Hypoxia-ischemia model in the 7-day-old rat: possibilities and shortcomings.** *Acta Pediatr Suppl* 1997;422:85–88
22. Pulera MR, Adams LM, Liu H, et al. **Apoptosis in a neonatal rat model of cerebral hypoxia-ischemia.** *Stroke* 1998;29:2622–2630
23. Bonfoco E, Krainc D, Ankarchoma M, Nicotera P, Lipton SA. **Apoptosis and necrosis: two distinct events induced respectively, by mild and intense insults with N-methyl-d-aspartate or nitric oxide/superoxide in cortical cell cultures.** *Proc Natl Acad Sci U S A* 1995;92:7162–7166
24. Kirino T. **Delayed neuronal death in the gerbil hippocampus following ischemia.** *Brain Res* 1982;239:57–69
25. Hope PL, Costello EB, Cady EB, et al. **Cerebral energy metabolism studied with phosphorous NMR spectroscopy in normal and birth-asphyxiated infants.** *Lancet* 1984;2:336–370
26. Azzopardi D, Wyatt JS, Cady EB, et al. **Prognosis of newborn infants with hypoxic/ischemic brain injury assessed by phosphorous magnetic resonance spectroscopy.** *Pediatr Res* 1989; 24:445–451
27. Lorek A, Takei Y, Cady EB, et al. **Delayed ("secondary") cerebral energy failure after acute hypoxia-ischemia in the newborn piglet: continuous 48-hour studies by phosphorous magnetic resonance spectroscopy.** *Pediatr Res* 1994;36:699–706